3. Margolis R, Spaide RF. A pilot study of enhanced depth imaging optical coherence tomography of the choroid in normal eyes. Am J Ophthalmol 2009;147:811–3.
4. Yoshida A, Hirokawa H, Ishiko S, Ogasawara H. Ocular circulatory changes following scleral buckling procedures. Br J Ophthalmol 1992;76:529–31.

Adaptive Optics Photoreceptor Imaging

Dear Editor:

In the present study, we investigated the cone packing density distribution along the horizontal meridian passing through the fovea in a population of young healthy subjects using a compact Adaptive Optics (AO) retinal camera (*rtx1*, Imagine Eyes, Orsay, France).

Nineteen healthy volunteer subjects (5 men and 14 women; age range, 24–38 years) participated in this study and gave a written informed consent. All subjects had 20/20 or better monocular best-corrected visual acuity and the spherical equivalent refractive errors ranged from −0.25 to −5.75 diopters (D) with astigmatism less than −1.50 D when referenced to the spectacle plane. The axial length (AxL) ranged between 22.61 and 26.29 mm. The protocol had approval of the local Ethical Committee and adhered to the tenets of Declaration of Helsinki. Exclusion criteria for this study included any ocular or systemic diseases.

Adaptive Optics imaging sessions were conducted after the pupils were dilated with 1 drop each of 0.5% tropicamide and 10% phenylephrine hydrochloride. A program provided by manufacturer correlated and averaged the captured image frames to reduce noise artefacts and produce a final image. Image analysis of the photoreceptor mosaic was performed using Image J (version 1.45a; NIH, Bethesda, MD). Cone density (cells/mm^2) was estimated within two 50×50 μm windows at specified eccentricities (250-, 420-, 760- and 1300-μm) from the foveal center (Fig 1; available http://aaojournal.org). The spectacle-corrected magnification factor (RMF_{corr}) was determined in all the eyes.

With the exception of the central fovea (<160 μm), the photoreceptor structure was well resolved in most of the eyes. Cones were in close proximity to each other at 200 μm from the foveal center; at increasing retinal eccentricities, cones tended to become progressively larger and the intercellular space was wider between cells, with rods intruding between cones (Fig 2; available at http://aaojournal.org), in accordance with the histologic studies of the human retina.[1] A variation in brightness between adjacent areas of cones was seen in all the eyes. The mean cone density was 50 574±6031 cells/mm^2 at 250 μm eccentricity, falling to 14 198±2114 cells/mm^2 at 1300 μm eccentricity (analysis of variance [ANOVA]; $P<0.05$). In general, subjects with higher cone density close to the foveal center had higher cone density at increasing eccentricities. The intersubject variability in parafoveal cone density distribution, estimated by the coefficient of variation, was within 15%.

Adaptive Optics technology opens a new frontier for the research in clinical Ophthalmology. The accurate measurements of retinal microscopic sized features in normal populations, according to age, refractive defects, etc., represents the basis for detecting early pathological changes of the photoreceptor layer. The cone density found in the present study could be considered representative of a healthy population of myopic adults. In previous works using AO-scanning laser ophthalmoscope (SLO), Li et al[2] found an average decline in cone density from ~120 000 to ~45 000 cell/mm^2 from 0.10– to 0.30–mm eccentricity from the foveal center in a population of 18 adult young subjects (23–43 years; AxL 22.86–28.31 mm). Chui et al[3] found an average cone density of ~35 000 cell/mm^2 at 0.5 mm, ~20 000 cell/mm^2 at 1.0 mm, and ~12 000 cell/mm^2 at 1.5 mm eccentricity from the fovea respectively in 11 subjects (21–31 years; AxL: 22.00–28.00 mm). Song et al[4] found a mean cone density of ~70 000 cell/mm^2 at 0.18 mm from the fovea falling to 37 000 cell/mm^2 and 19 000 cell/mm^2 at 0.5- and 1.1-mm eccentricity respectively in a population of 10 young adults (22–35 years; AxL, 22.10–26.30 mm).

We based our method of cone counting on the results of a previous work by Hirsch and Miller.[5] The authors demonstrated that a 56×56 μm was less subject to error than smaller window sizes when estimating cone density across increasing eccentricity from the fovea. Previous authors recently used a 50×50 μm sampling window to locate cone photoreceptor positions,[4] further showing a high repeatability in cone density estimates taken 6 months apart at the same retinal location.

Data on populations of healthy eyes are fundamental in characterizing the density, distribution, and appearance of normal photoreceptor cells in vivo. This will permit measurement of the normal ranges, which allows comparison with pathological photoreceptors, even in early stages of retinal diseases.

Marco Lombardo, MD, PhD
Giuseppe Lombardo, MEng, PhD
Pietro Ducoli, MD
Sebastiano Serrao, MD, PhD
Rome, Italy

References

1. Curcio CA, Sloan KR, Kalina RE, Hendrickson AE. Human photoreceptor topography. J Comp Neurol 1990;292:497–23.
2. Li KY, Tiruveedhula P, Roorda A. Intersubject variability of foveal cone photoreceptor density in relation to eye length. Invest Ophthalmol Vis Sci 2010;51:6858–67.
3. Chui TYP, Song H, Burns S. Adaptive-optics imaging of human cone photoreceptor distribution, J Opt Soc Am A 2008;25:3021–9.
4. Song H, Chui TYP, Zhong Z, et al. Variation of cone photoreceptor packing density with retinal eccentricity and age. Invest Ophthalmol Vis Sci 2011;52:7376–84.
5. Hirsch J, Miller WH. Does cone positional disorder limit resolution? J Opt Soc Am A 1987;4:1481–92.

General Correspondence

Descemet's Stripping Automated Endothelial Keratoplasty

Dear Editor:

We read with interest the article entitled, "Graft rejection after Descemet's stripping automated endothelial keratoplasty"[1] by Li et al. The article presents important insight

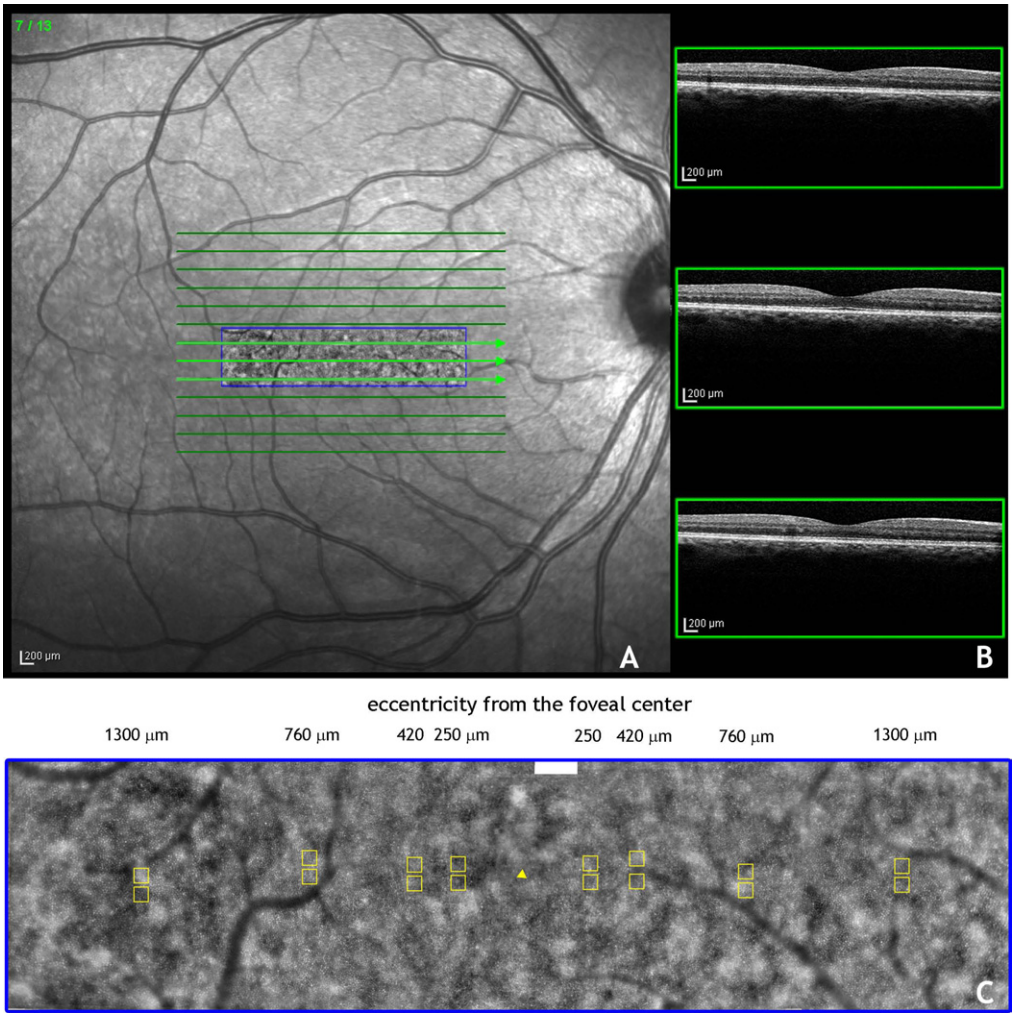

Figure 1. The right eye of a 31-year-old woman (axial length, 23.89 mm; spherical equivalent refraction −1.00 D). **A**, The scanning laser ophthalmoscope (SLO) image with the superimposed Adaptive Optics (AO) retinal montage. The horizontal AO montage subtends an area of 3.67×1.46 mm. **B**, The optical coherence tomography (OCT) images corresponding to the 3 horizontal raster lines passing through the foveal pit (yellow triangle), showing a normal appearance of the retinal tissue. In **C**, the photoreceptor mosaic of the parafoveal region. The yellow squares indicate the 50×50 μm fixed windows used to estimate cone density. Eccentricity was computed as the distance between the center of each window and the foveal center. We made sure not to perform cone photoreceptors counting on regions with vessels or defects in the image quality: an underestimation of density may indeed occur when regions of missing data (e.g., blood vessels or dark areas likely due to defects in the image quality) are present into the sampling window.

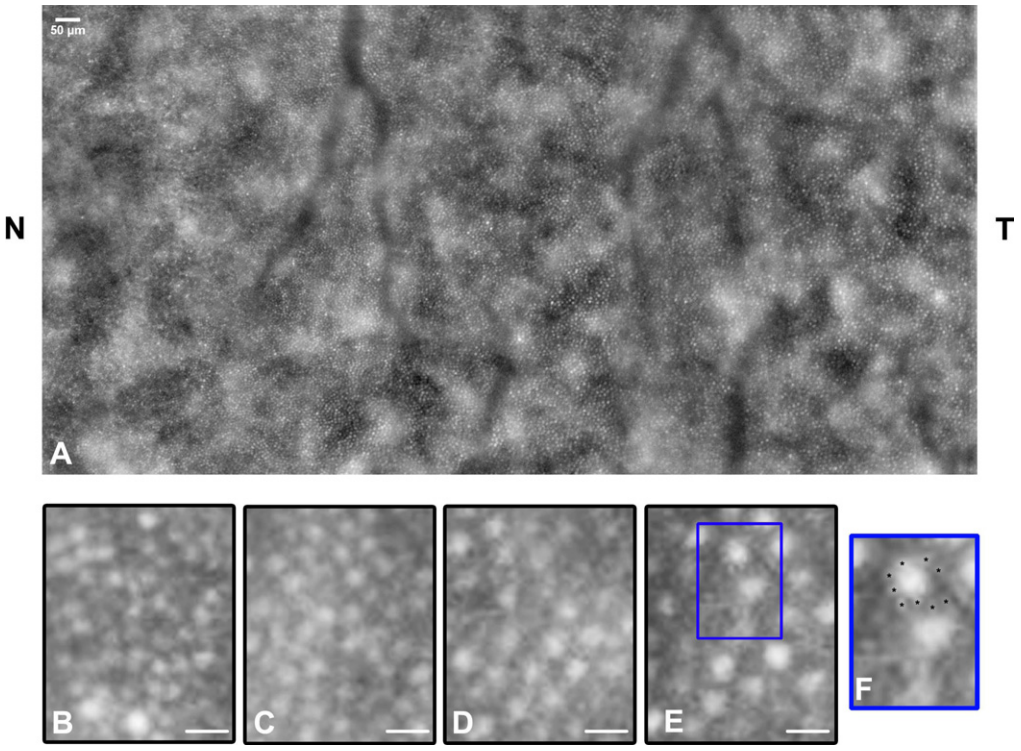

Figure 2. **A**, The cone photoreceptor mosaic along the temporal meridian of the parafoveal region in the left eye of 1 subject (32-year-old woman). The Adaptive Optics (AO) montage includes an area between 0.19 mm and 1.7 mm eccentricities temporally from the foveal center. Differences in the reflectance across adjacent cone photoreceptors are often observed when imaging the photoreceptor layer. Although the origin of the cell-to-cell variability in cone reflectance remains unclear, it has been mainly related to the cell biology, including the cone outer segment pigment density. In **B**, **C**, **D**, and **E**, high-magnification images (45×90 μm) of the photoreceptor layer taken at increasing eccentricities from the foveal center: 280 μm, 560 μm, 1250 μm, and 1600 μm, respectively. Eccentricity dependent changes in cone morphology and packing are evidenced: cones are more densely packed close to the fovea and the intercone distance widens at increasing eccentricities (scale bar, 10 μm). **F**, A detail of the inset in **E**: rods could be faintly visualized as round cells (asterisks) surrounding the larger cones, as also recently shown by Dubra et al using an AO-SLO (Biomed Opt Expr 2011;2:1864). N = nasal; T = temporal.